Cancer Research

Regulation of Insulin-like Growth Factor–Mammalian Target of Rapamycin Signaling by MicroRNA in Childhood Adrenocortical Tumors

Mabrouka Doghman[1,2], Abeer El Wakil[1,2], Bruno Cardinaud[1,2], Emilie Thomas[3], Jinling Wang[4], Wei Zhao[5], Maria Helena C. Peralta-Del Valle[6], Bonald C. Figueiredo[6], Gerard P. Zambetti[4], and Enzo Lalli[1,2]

Abstract

MicroRNAs (miRNAs) act at the posttranscriptional level to control gene expression in virtually every biological process, including oncogenesis. Here, we report the identification of a set of miRNAs that are differentially regulated in childhood adrenocortical tumors (ACT), including miR-99a and miR-100. Functional analysis of these miRNAs in ACT cell lines showed that they coordinately regulate expression of the insulin-like growth factor–mammalian target of rapamycin (mTOR)–raptor signaling pathway through binding sites in their 3′-untranslated regions. In these cells, the active Ser^{2448}-phosphorylated form of mTOR is present only in mitotic cells in association with the mitotic spindle and midbody in the G_2-M phases of the cell cycle. Pharmacologic inhibition of mTOR signaling by everolimus greatly reduces tumor cell growth *in vitro* and *in vivo*. Our results reveal a novel mechanism of regulation of mTOR signaling by miRNAs, and they lay the groundwork for clinical evaluation of drugs inhibiting the mTOR pathway for treatment of adrenocortical cancer. *Cancer Res; 70(11); 4666–75. ©2010 AACR.*

Introduction

Adrenocortical tumors (ACT) in children may occur sporadically or in association with other types of neoplasms in the context of multiple neoplasia syndromes linked to germline tumor suppressor gene mutations (1). The incidence of these tumors is highest during the first 3 years of life and is several times more frequent in southern Brazil than in the rest of the world (2). In that geographic region, childhood ACTs are almost invariably associated with the germline R337H tumor protein p53 (*TP53*) mutation (3). These tumors are believed to be derived from the fetal adrenal cortex because of their age distribution, their pattern of hormone secretion, and their molecular phenotype (2, 4).

Although the most common genetic basis of childhood ACT is germline *TP53* mutations with loss of heterozygosity (LOH) in the tumor, our knowledge of the molecular pathogenesis of these neoplasms is still limited. A very frequent feature is represented by LOH of the distal region of the short arm of chromosome 11, with preferential expression of the imprinted paternal allele and overexpression of the insulin-like growth factor-II (IGF-II; refs. 4, 5). IGF-II signaling through the IGF-IR is thought to represent an important mechanism for ACT growth and a relevant therapeutic target (6, 7). In addition, amplification and overexpression of the nuclear receptor steroidogenic factor-1 (NR5A1) is thought to play an important role in ACT pathogenesis (8, 9). Last, a study of protein-coding mRNAs found a distinct pattern of their expression in childhood ACT compared with normal adrenal cortex and also identified a set of transcripts whose expression is related to prognosis (10).

MicroRNAs (miRNAs) belong to a class of small noncoding RNAs of ~21-nucleotide length that control gene expression at the posttranscriptional level. In their mature form, miRNAs recognize by base-pairing sequences in the 3′-untranslated region (UTR) of protein-coding transcripts, leading to translational repression or mRNA degradation (11). miRNAs are involved in virtually every biological process, from development to viral infection, and are also associated with oncogenesis (12). In addition, a great number of known miRNAs are located at fragile sites and genomic regions implicated in cancer (13).

As part of our effort to elucidate the genetic determinants of childhood ACT, in this study, we analyzed the miRNA expression pattern of childhood ACT. A group of miRNAs was found to be differentially expressed in ACT compared with normal adrenal. We focused our functional analysis on miR-99a and miR-100, which are significantly downregulated in ACT and share the same seed sequence. Among the predicted targets

Authors' Affiliations: [1]Institut de Pharmacologie Moléculaire et Cellulaire; [2]Université de Nice-Sophia Antipolis, Valbonne, France; [3]Programme Carte d'Identité des Tumeurs, Ligue Nationale Contre Le Cancer, Paris, France; Departments of [4]Biochemistry and [5]Biostatistics, St. Jude Children's Research Hospital, Memphis, Tennessee; and [6]Instituto de Pesquisa Pelé Pequeno Principe and Faculdades Pequeno Principe, Curitiba PR, Brazil

Note: Supplementary data for this article are available at Cancer Research Online (http://cancerres.aacrjournals.org/).

Current address for B. Cardinaud: Université Bordeaux 2, Bordeaux, France.

M. Doghman and A. El Wakil contributed equally to this work.

Corresponding Author: Enzo Lalli, Institut de Pharmacologie Moléculaire et Cellulaire, 660 route des Lucioles, 06560 Valbonne, France. Phone: 33-4-93-95-77-55; Fax: 33-4-93-95-77-08; E-mail: ninino@ipmc.cnrs.fr.

doi: 10.1158/0008-5472.CAN-09-3970

of these miRNAs, transcripts are found that encode key components of the IGF (IGF-IR) and mammalian target of rapamycin (mTOR and raptor) signaling pathways. Here, we show that mTOR signaling is activated in ACT and that miR-99a and miR-100 regulate expression of mTOR, raptor, and IGF-IR in adrenocortical cancer cells. Moreover, the specific mTOR inhibitor RAD001 (everolimus) potently suppresses adrenocortical cancer cell proliferation *in vitro* and when grown as xenografts in immunodeficient mice. These data reveal a novel layer of regulation of IGF and mTOR signaling by miRNAs and show that mTOR inhibition represents a potential new therapeutic tool in adrenocortical cancer.

Materials and Methods

Human subjects

All patients and normal subjects gave their informed consent to this study, which was approved by the Ethical Committees of Pequeno Principe and St. Jude Children's Research Hospitals. Patients' clinical data are reported in Supplementary Table S1. Normal adrenal glands were obtained with Institutional Review Board approval as discarded tissue from cases of Wilms' tumor. These patients, whose age ranged from 2 to 6 years, had not received chemotherapy before surgery. Normal adrenal cortex samples were isolated by an American Board–certified pathologist, snap frozen in liquid nitrogen, and processed for RNA extraction as described below.

miRNA expression studies

RNA was extracted from frozen tissue samples using the miRNeasy Mini kit (Qiagen). Total RNA (200 ng) from each sample was labeled and hybridized to human V2 microarrays (Agilent), following the manufacturer's procedures. The original expression data were first thresholded in such a way that any value less than the threshold was assigned to be equal to the threshold and any value above the threshold was left intact. The thresholded data were then $\log_2$ transformed and used for further analysis. We used the Kruskal-Wallis test to compare the median expression levels between the normal and ACT samples in each probe set. The probe sets with P value of <0.01 and signals present in at least 10 samples were used to make the heat map plot. The threshold used in this study is 1. All analyses were implemented in R version 2.6.2. Microarray data were deposited in the Gene Expression Omnibus database under record number GSE19856. Taqman reverse transcription-quantitative PCR (qPCR; Applied Biosystems) was used to confirm the expression levels of the miRNAs identified as differentially expressed by microarray plus the let-7a miRNA as a control. *RNU48* was used as a reference gene for miRNA qPCR. For target gene identification, the Targetscan database (http://www.targetscan.org/) was interrogated.

Immunoblotting

Protein extracts were prepared by homogenization of tissues and cells in Laemmli buffer [50 mmol/L Tris-HCl (pH 6.8), 50% glycerol, 2% SDS, 0.02% bromphenol blue] containing 5% β-mercaptoethanol. Proteins were separated by SDS-PAGE and transferred to a nitrocellulose membrane (Schleicher & Schuell). Primary antibodies used were anti-mTOR (Abcam), anti–phospho-mTOR (Ser^{2448}; Cell Signaling Technology), anti-raptor (Cell Signaling Technology), anti-rictor (Cell Signaling Technology), anti–IGF-IRβ (Cell Signaling Technology), and anti-p42/p44 mitogen-activated protein kinases (Cell Signaling Technology). Immunoblot was performed using a chemiluminescence system for protein detection (GE Healthcare). Bands on blots were quantified using the ImageJ software (http://rsbweb.nih.gov/ij/).

mTOR activity enzyme immunoassay

Tissue lysates were prepared by homogenization in lysis buffer [50 mmol/L Tris-HCl (pH 7.4), 100 mmol/L NaCl, 50 mmol/L β-glycerophosphate, 10% glycerol, 1% Tween 20, 1 mmol/L EDTA, 20 nmol/L microcystin-LR, 25 mmol/L NaF] supplemented with protease inhibitor cocktail (Sigma-Aldrich). After centrifugation at 16,000 × g for 20 minutes to eliminate debris, total protein concentration in the lysates was adjusted to 3 mg/mL and 0.8 mL of the lysates was incubated with anti-mTOR agarose beads (Abcam) for 2 hours at 4°C. The immunoprecipitates were then washed twice with lysis buffer, and mTOR activity in the tissue lysates was measured with an immunoenzymatic assay (K-LISA mTOR Activity kit, Calbiochem) using a recombinant GST-p70S6K protein as a substrate, following the manufacturer's instructions.

Immunohistochemistry

Immunohistochemistry was performed on tumor paraffin sections after antigen retrieval using antibodies directed against phospho-mTOR (Ser^{2448}) and phospho–ribosomal protein S6 (RPS6; Ser$^{240/244}$; Cell Signaling Technology). Immunoreactivity was graded with scores from 0 to +++, which corresponded to negative, weak, intermediate, or strong staining intensity.

Transfections and luciferase assay

mTOR (nucleotides 7782–8707 of sequence NM_004958), raptor (nucleotides 4957–5361 of sequence NM_020761), and IGF-IR (nucleotides 9543–9833 of sequence NM_000875) 3′-UTR sequences were PCR amplified from a HeLa cell cDNA library (Clontech) using the primers shown in Supplementary Table S2 and cloned in the *Not*I-*Xho*I sites of the double-luciferase psiCHECK-2 vector (Promega) appended to the *Renilla* luciferase gene. Deletions in the 3′-UTR–predicted miR-99a/miR-100 binding sites were made by QuikChange mutagenesis (Stratagene). HEK 293T cultured in DMEM (4.5 g/L glucose) supplemented with 10% FCS and antibiotics in 96-well white plates (Costar) were reverse transfected in triplicate with 3′-UTR reporter constructs using Lipofectamine 2000 (Invitrogen) and pre-miR-99a, pre-miR-100, or negative control #1 precursor molecules (Ambion). *Renilla* and firefly luciferase activities were measured with a Luminoskan Ascent (Thermo Labsystems) luminometer. For each sample, *Renilla* luciferase activity was normalized by firefly luciferase activity. Each experiment was repeated three times.

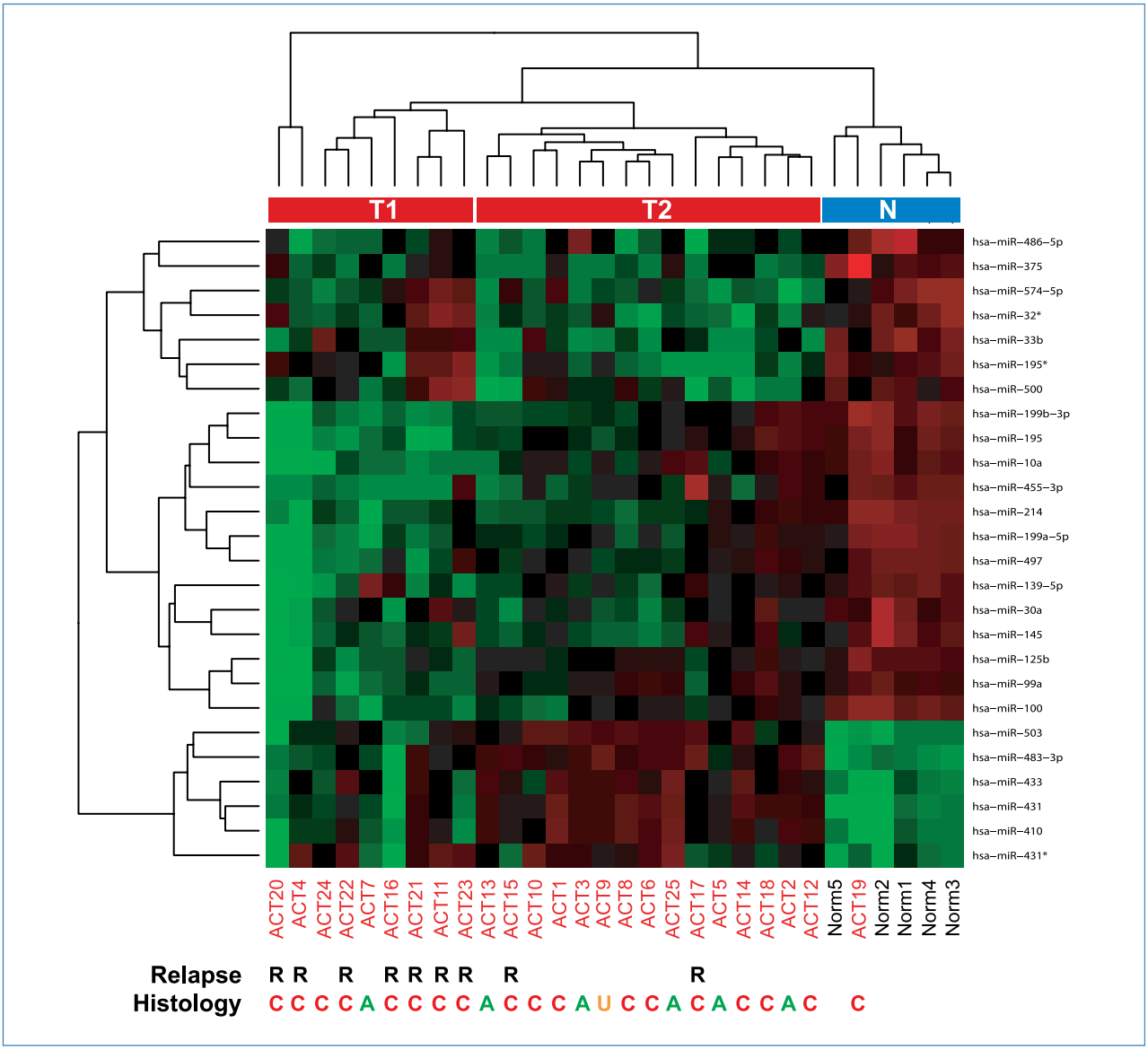

Figure 1. Identification of differentially expressed miRNAs in childhood ACT. Heat map plot of significantly differentially expressed miRNAs in childhood ACT compared with normal adrenal cortex. R, patients with relapse; A, adenoma (Weiss index <3); C, carcinoma (Weiss index ≥3); U, unknown histologic type. Unsupervised clustering divides tumor miRNA expression profiles into two distinct groups (T1 and T2). N, normal adrenal cluster.

ACT cell line culture

H295R cells were cultured in DMEM/F12 supplemented with 2% NuSerum (Becton Dickinson), 1% ITS+ (Becton Dickinson), and antibiotics. SW-13 cells were cultured in DMEM/F12 medium supplemented with 10% FCS (Invitrogen) and antibiotics. HAC15 cells were cultured in DMEM/F12 supplemented with 10% cosmic calf serum (HyClone), 1% ITS+, and antibiotics. Primary cells isolated from a pediatric ACT were cultured as described (14). As a method of authentication, the karyotype of cell lines and the steroid secretion profile of H295R cells were periodically tested.

miRNA knockdown

For endogenous miRNA knockdown, 1×10^5 cells per well were seeded in 12-well plates and transfected with miR-100–specific or scramble control miRCURY LNA knockdown probes (Exiqon) using Lipofectamine 2000. Forty-eight hours after transfection, levels of endogenous mTOR, raptor, and IGF-IR were analyzed by Western blotting.

Immunofluorescence

Immunofluorescence was performed on formaldehyde-fixed H295R cells cultured on glass slides using the anti-mTOR (Cell Signaling Technology), anti–phospho-mTOR (Ser^{2448}), and anti–β-tubulin (Sigma-Aldrich) as primary antibodies revealed with Alexa594- and Alexa488-labeled secondary antibodies (Invitrogen). 4′,6-Diamidino-2-phenylindole (DAPI) was used as nuclear counterstain. Images were acquired with a Zeiss Axioplan 2 fluorescence microscope

coupled to a digital charge-coupled device camera and processed using ImageJ.

Xenografts

H295R cells (6×10^6) were inoculated s.c. into the right flank of 4-week-old female NOD/SCID/γ_c^{null} mice. Three weeks later, when palpable tumors appeared, injected mice were randomly assigned to three groups of eight animals treated with placebo or with a preparation of RAD001 for oral administration (3 and 10 mg/kg/d). Drugs were administered by gavage and tumor growth was monitored by measuring with a Vernier caliper and calculating tumor volume (length × width × height × π/6). After the end of treatment, animals were euthanized according to the institutional animal care and use committee protocol. Xenografts were excised, weighted, and either frozen in OCT or formaldehyde fixed and included in paraffin for histologic studies. Blood vessels were stained with Texas red–conjugated tomato lectin (Vector), and immunohistochemistry for phospho-RPS6 was performed as described before (see Immunohistochemistry section).

Results

A set of miRNAs is differentially expressed in childhood ACT

We investigated miRNA expression in a series of 25 ACT (patients' clinical data are reported in Supplementary Table S1) and compared it with a group of 5 normal adrenocortical

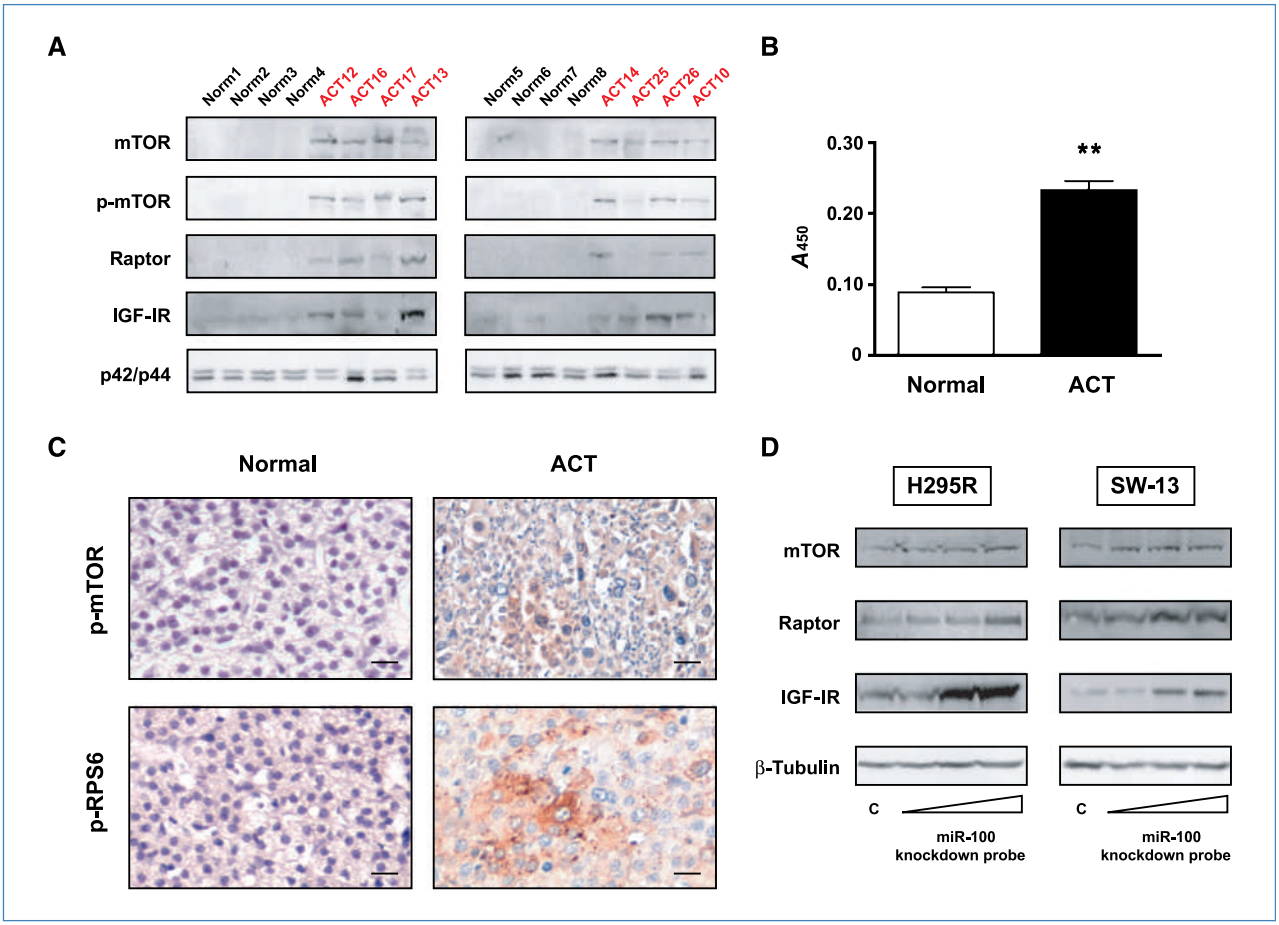

Figure 2. mTOR signaling is activated in childhood ACT, and knockdown of endogenous miR-100 regulates expression of mTOR, raptor, and IGF-IR proteins in ACT cells. A, immunoblot showing expression of mTOR, phospho-mTOR (Ser^{2448}), raptor, and IGF-IR proteins in a series of eight ACTs (ACT10, ACT12, ACT13, ACT14, ACT16, ACT17, ACT25, and ACT26; see Supplementary Table S1 for patients' clinical data) and eight normal adrenal cortex samples. p42/p44 expression is shown as loading control. Quantification of immunoblot results is shown in Supplementary Fig. S3. B, mTOR kinase activity against recombinant GST-p70S6K was measured in eight ACTs (ACT7, ACT9, ACT11, ACT15, ACT16, ACT27, ACT28, and ACT29; see Supplementary Table S1 for clinical data) and three normal adrenal cortex samples by enzyme immunoassay. **, $P < 0.01$, Student's t test. C, top, immunohistochemistry showing strong diffuse expression of phospho-mTOR (Ser^{2448}) in one ACT sample (ACT30; see Supplementary Table S1 for patients' clinical data); bottom, focal phospho-RPS6 (Ser$^{240/244}$) staining in another ACT sample (ACT32). Magnification, ×40. Scale bars, 20 μm. Quantification of immunohistochemical results for each patient analyzed is shown in Supplementary Table S3. D, H295R (left) and SW-13 (right) tumor adrenocortical cells were transfected with increasing concentrations (10, 25, and 50 nmol/L) of miR-100 knockdown probe or scramble control (50 nmol/L). Expression of endogenous mTOR, raptor, and IGF-IR proteins was revealed by immunoblot 48 h after transfection. β-Tubulin expression is shown as loading control.

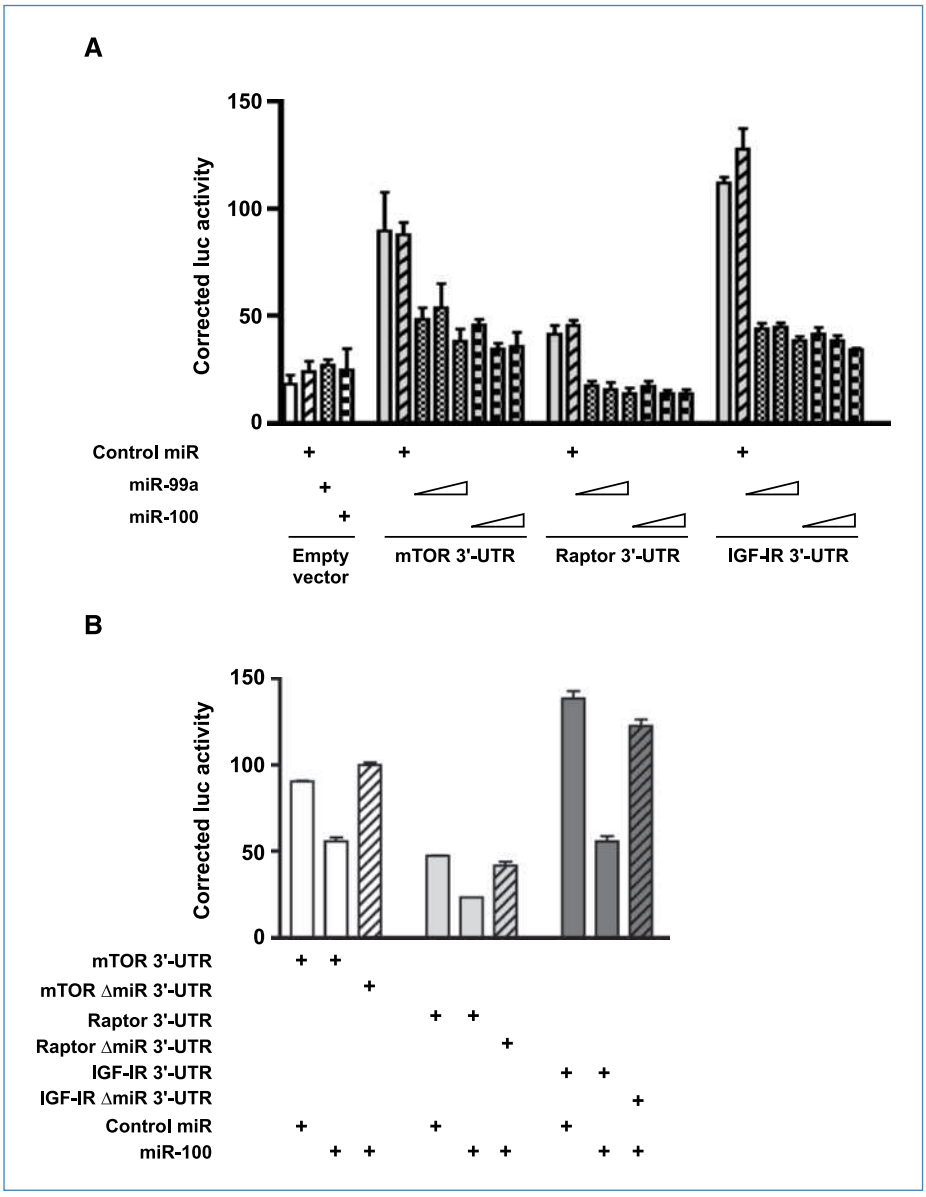

Figure 3. Regulation of mTOR, raptor, and IGF-IR expression by miR-99a/miR-100 through their 3′-UTRs. A, increasing concentrations of miR-99a and miR-100 pre-miRs (5, 10, and 25 nmol/L) repress expression of *Renilla* luciferase harboring mTOR, raptor, and IGF-IR 3′-UTR sequences in transfected HEK 293T cells. No significant effect was detected for 25 nmol/L control pre-miR. The weak activity of the transfected empty vector (psiCHECK-2) was not affected by cotransfection with any of the pre-miRs. B, pre-miR-100 (50 nmol/L) efficiently represses activity of luciferase-mTOR, luciferase-raptor, and luciferase–IGF-IR 3′-UTRs, whereas constructs with deleted miRNA binding sites for each 3′-UTR are not sensitive to repression by pre-miR-100.

samples from age-matched subjects. Significant modulation of expression in ACT was found for 26 miRNAs with a P value of <0.01. These miRNAs are shown in the heat map in Fig. 1. The majority (77%) of the differentially expressed miRNAs was downregulated in ACT compared with normal adrenal cortex. Differentially regulated expression of all these miRNAs in ACT compared with normal adrenal cortex was confirmed by Taqman qPCR, whereas expression of the let-7a miRNA, which was not detected as differentially expressed in the microarray study, was not significantly different (Supplementary Fig. S1).

ACT and normal samples were clustered into two distinct groups by unsupervised analysis, except for a single ACT sample whose miRNA expression profile clustered together with the normal group. Further analysis showed that inside the ACT cluster, two subclusters were present (T1, more distant from the normal group, and T2, closer to the normal group; see Fig. 1). Probability of relapse was significantly associated with localization in the T1 subcluster (P = 0.002, Fisher's exact test), whereas histologic type (adenoma or carcinoma) was not significantly associated with any group of samples (P = 0.35, Fisher's exact test). The expression of no single miRNA could perfectly discriminate cases with relapse from cases without relapse.

mTOR, raptor, and IGF-IR are overexpressed in ACT and upregulated by miR-100 knockdown in ACT cell lines

Among the most significantly downregulated miRNAs in ACT were miR-99a and miR-100, which share the same seed

sequence and are predicted to target the 3′-UTRs of pivotal components of IGF (IGF-IR) and mTOR [FRAP1 (mTOR) and RPTOR (raptor)] signaling (Supplementary Fig. S2). Although the importance of IGF signaling in ACT is well known (6, 7, 15), no data exist yet about the involvement of the mTOR pathway in the pathogenesis of ACT. We studied the expression of mTOR (and its active phosphorylated form at Ser^{2448}), raptor, and IGF-IR proteins in a series of ACT samples and compared it with normal adrenal cortex samples. mTOR, phospho-mTOR (Ser^{2448}), raptor, and IGF-IR protein levels were significantly higher in ACT (Fig. 2A; Supplementary Fig. S3). Conversely, the other mTOR-associated protein rictor was not detectable either in normal adrenal samples or in ACT (data not shown). mTOR activity was also significantly higher in ACT compared with normal adrenocortical tissue (Fig. 2B). Finally, phosphorylation of mTOR at Ser^{2448} and of RPS6 as markers of active mTOR signaling was detected in ACT by immunohistochemistry (Fig. 2C). Quantification of immunohistochemical results is shown in Supplementary Table S3. Taken together, these results show that mTOR signaling is active in ACT. To investigate whether downregulation of endogenous miR-100 can modulate the levels of mTOR, raptor, and IGF-IR proteins, we transfected a specific miR-100 knockdown probe or a control probe into two different human adrenocortical cell lines (H295R and SW-13) and detected a dose-dependent increase in mTOR, raptor, and IGF-IR protein expression only after miR-100–specific knockdown (Fig. 2D).

miRNAs of the miR-100 family regulate the expression of mTOR, raptor, and IGF-IR through their 3′-UTRs

With the purpose to assess whether miR-99a and miR-100 can directly regulate the expression of mTOR, raptor, and IGF-IR, we fused portions of the 3′-UTR sequences of these genes harboring predicted binding sites for miR-99a/miR-100 to the luciferase reporter gene and performed transfections in HEK 293 cells in the presence of synthetic miR-99a, miR-100, or control miRNA precursors. As shown in Fig. 3A, the addition of mTOR and IGF-IR 3′-UTR sequences conferred high expression to the luciferase gene, whereas the raptor 3′-UTR had only a modest effect on luciferase activity. Although the expression of all constructs, including the empty vector, was insensitive to the effect of a high concentration (25 nmol/L) of the control miRNA precursor, miR-99a and miR-100 efficiently repressed the expression of luciferase fused to the mTOR and IGF-IR 3′-UTRs in a dose-dependent fashion, starting from a concentration of 5 nmol/L. They also repressed the expression of luciferase-raptor 3′-UTR to baseline levels. Importantly, even the highest concentrations of miR-99a and miR-100 precursors (25 nmol/L) had no effect on the expression of luciferase, indicating that the miRNA effect was specifically mediated by the sequences appended to the 3′ end of the luciferase coding region (Fig. 3A). Moreover, IGF-IR, mTOR, and raptor 3′-UTRs deleted of their predicted miR-99a/miR-100 binding sites were insensitive to repression by a high concentration (50 nmol/L) of miR-100 precursor that efficiently repressed the wild-type constructs (Fig. 3B).

The phosphorylated, active form of the mTOR kinase (phospho-Ser^{2448}) is specifically enriched in mitotic tumor adrenocortical cells

Considering the potential effect of miRNAs of the miR-100 family in modulating the expression of proteins involved in mTOR signaling, we explored the role of this pathway in regulating the proliferation of ACT cells. We started by studying the cellular localization of mTOR and its Ser^{2448}-phosphorylated, active form. Whereas mTOR is distributed in the cytoplasm of ACT H295R cells, phospho-mTOR is strikingly enriched in mitotic cells (Supplementary Fig. S4). In prophase, a bright phospho-mTOR staining appeared among condensed chromosomes,

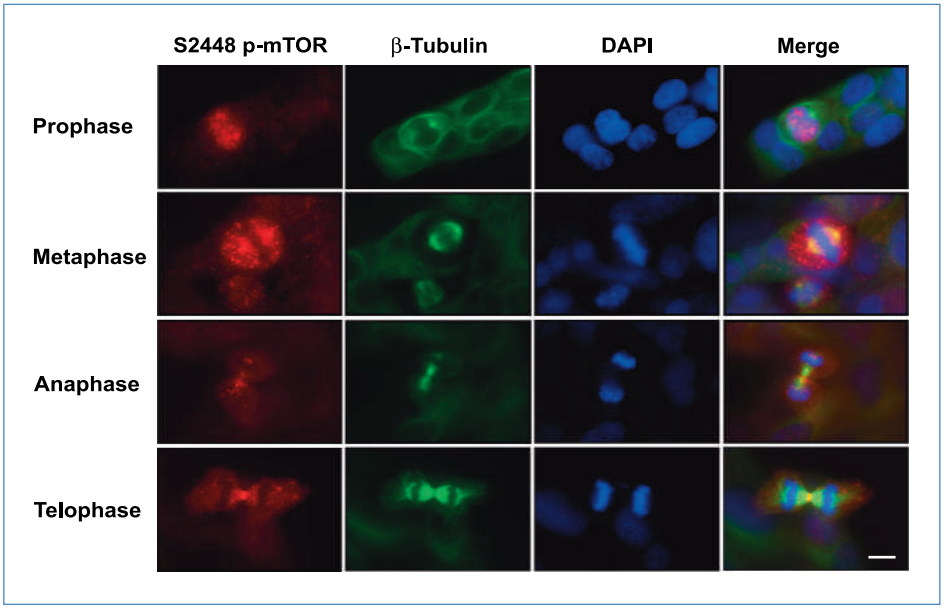

Figure 4. Phospho-mTOR (Ser^{2448}) is specifically expressed during mitosis in human ACT cells. The expression of phospho-mTOR (Ser^{2448}; in red) was revealed by immunofluorescence during the different stages of mitosis in H295R cells. β-Tubulin expression is shown in green and DAPI staining in blue. Magnification, ×100. Scale bar, 10 μm.

which at metaphase partly colocalized with the mitotic spindle, being also present in a bright dot-like pattern in the cytoplasm of mitotic cells (Fig. 4). Starting from anaphase, the phospho-mTOR signal moved to the midzone and progressively concentrated at the midbody in the cleavage furrow during telophase and cytokinesis (Fig. 4).

Blockage of mTOR activity inhibits ACT cell proliferation *in vitro* and xenograft growth

Because of the effects of mTOR signaling on cell growth and proliferation, mTOR inhibitors derived from the macrolide rapamycin are being used in the chemotherapy of different types of cancer (16). Because mTOR signaling is activated in ACT, we studied the effect of the mTOR inhibitor RAD001 (everolimus) on the proliferation of ACT cells H295R and SW-13. The drug significantly inhibited proliferation of both cell lines, showing a more potent effect on SW-13 than on H295R cells (IC_{50}, $10^{-8.9}$ mol/L versus $10^{-8.1}$ mol/L; Fig. 5A). RAD001 also inhibited the proliferation of primary childhood ACT cells (14), with an IC_{50} of $10^{-9.2}$ mol/L, and of the HAC15 cell line, derived from a pediatric adrenocortical carcinoma (17), with an IC_{50} of $10^{-8.6}$ mol/L (Fig. 5A).

We then measured the capacity of RAD001 to inhibit the growth of H295R cells injected as xenografts into nonobese diabetic/severe combined immunodeficient (NOD/SCID) mice. The drug (10 mg/kg/d) significantly inhibited xenograft growth compared with placebo treatment, without inducing detectable side effects on mice (Fig. 5B). A lower RAD001 dose (3 mg/kg/d) was not active (data not shown). Tumor weight and the number of mitoses per high-power microscopic field were also significantly lower in RAD001-treated animals (Supplementary Fig. S5A and B). As expected, RAD001 treatment potently reduced phospho-RPS6 expression in the xenografts and also reduced blood vessel number and extension (Supplementary Fig. S5C). In addition, we could detect thrombogenesis in tumor vasculature (Supplementary Fig. S5C), as described previously in other animal tumor models (18).

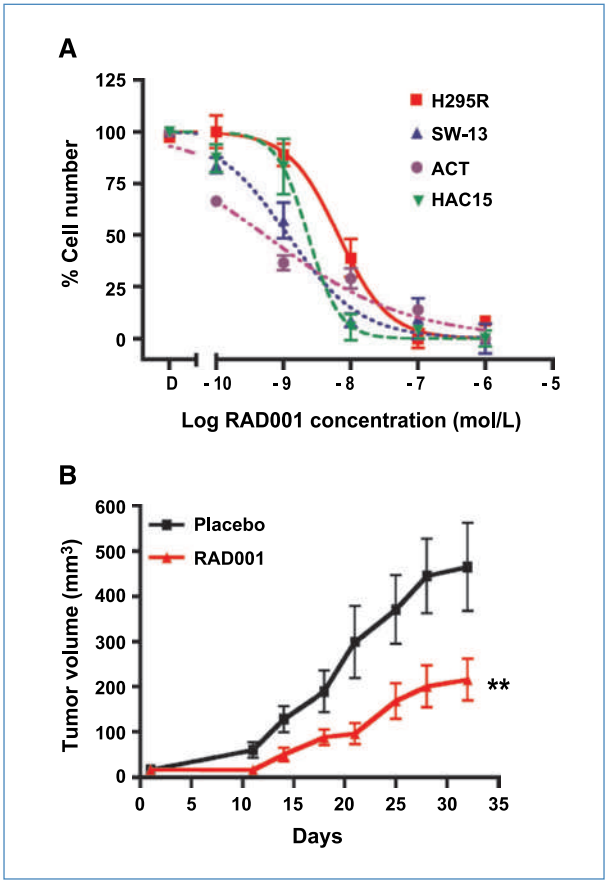

Figure 5. The rapamycin analogue RAD001 inhibits ACT cell growth *in vitro* and *in vivo*. A, H295R (red squares), SW-13 (blue triangles), primary ACT (purple circles), and HAC15 (green triangles) cells were cultured in 24-well plates in the presence of DMSO or of increasing concentrations of RAD001. Cells were counted after 6 d of culture in the presence of the drug. Points, mean; bars, SE. Data were generated from three different experiments each performed in duplicate. B, H295R xenograft growth in NOD/SCID/γ_c^{null} mice treated with placebo (black squares) or with RAD001 (10/mg/kg/d; red triangles). Points, mean; bars, SE. Tumor growth was significantly different in animals treated with the drug. **, $P < 0.01$, paired *t* test.

Discussion

Here, we have shown that the expression of a distinct set of miRNAs is differentially regulated in childhood ACT compared with normal adrenal cortex. Interestingly, unsupervised clustering revealed that miRNA profiles could distinguish between two groups of ACT in our series, one of which (T1 in Fig. 1) was associated with the risk of relapse. These data need to be validated on a larger series of cases. Consistently with previous results in other types of cancer (19), the majority of the differentially expressed miRNAs in ACT was downregulated compared with normal adrenal. Conversely, one miRNA that was found to be highly upregulated in ACT was miR-483-3p. The gene encoding this miRNA lies within an intron of the *IGF-II* gene in 11p15, which is overexpressed at high frequency in childhood ACT (4, 5). Further studies are required to assess the potential role of miR-483-3p overexpression in ACT pathogenesis. Three among the differentially expressed miRs (miR-503, miR-214, and miR-375) were also identified in a study of the miRNA expression profiles in adult ACT, with miR-503 and miR-375 displaying a significantly different expression in carcinomas compared with functioning adenomas (20). Moreover, another recent study described downregulation of miR-195 (which is also downregulated in ACT in our series) and upregulation of miR-483-5p (which is derived from the same precursor as miR-483-3p) as potential prognostic markers in adult ACT (21).

We focused our functional analysis on miR-99a and miR-100, which are among the most highly downregulated miRNAs in ACT. They share the same seed sequence, which suggests that they can regulate a common set of target mRNAs. Here, we show that in ACT cells these miRNAs regulate IGF-IR and mTOR signaling cascades at multiple levels through modulation of the expression of key proteins implicated in those pathways (Fig. 6). Previous reports have shown the importance of the IGF–IGF-IR pathway in the regulation of adrenocortical

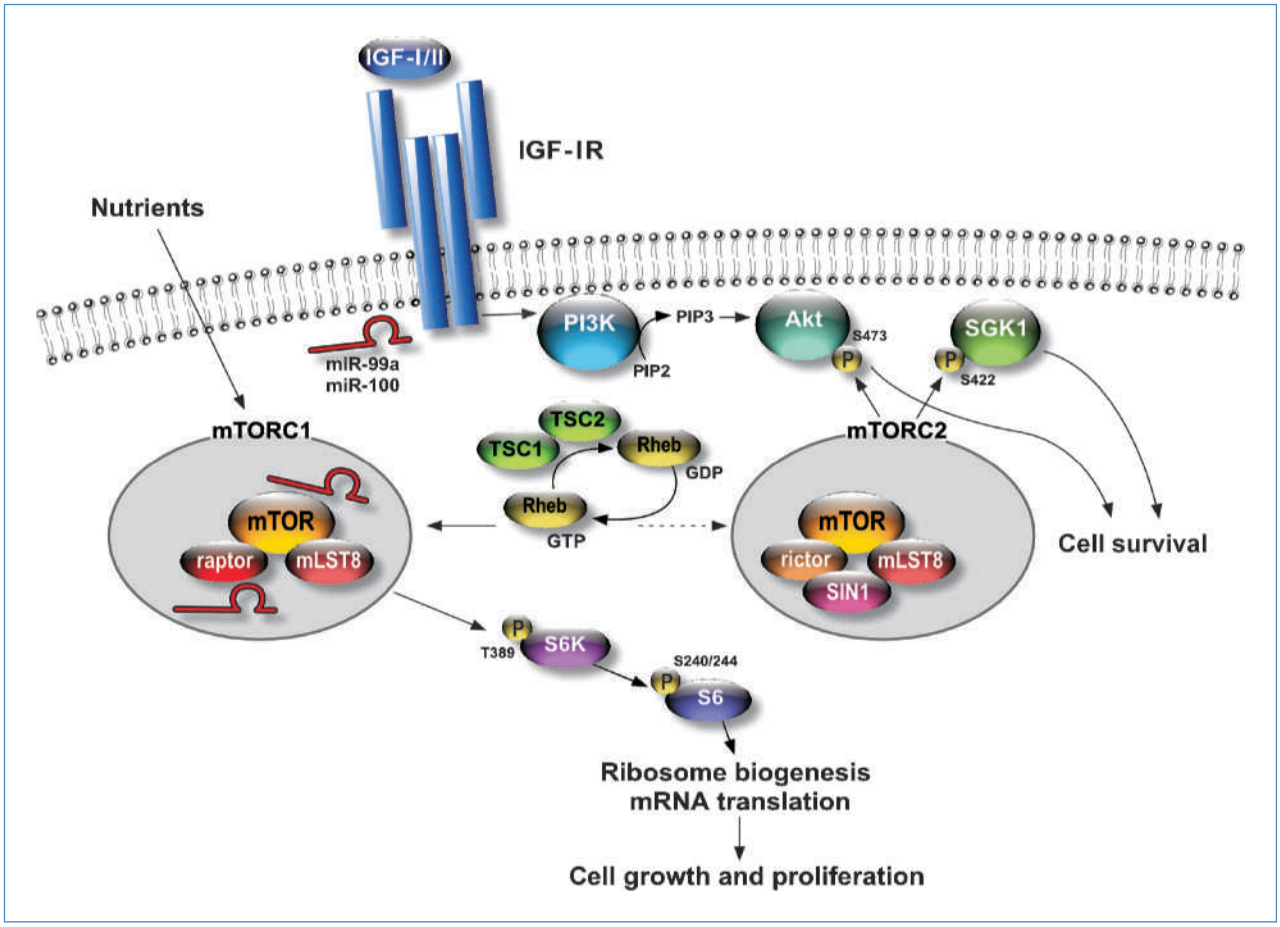

Figure 6. miR-99a/miR-100 regulate IGF-mTOR signaling at multiple levels. A simplified view of IGF-mTOR signaling. Key targets of miR-99a/miR-100 (indicated in red) regulation are shown.

cancer cell proliferation and the efficacy of targeting this pathway in preclinical models of the disease (6, 7, 15). Here, we have shown that IGF-IR levels are upregulated in ACT and that miR-99a/miR-100 can regulate its expression acting on a target site in the 3′-UTR of its mRNA. These data are consistent with previous findings showing overexpression of IGF-IR mRNA in ACT (6). In these tumors, very high IGF-II mRNA expression often does not translate into the production of a biologically active protein (10). High IGF-IR expression is then likely to play a pivotal role in the activation of the IGF pathway in these tumors.

Studies analyzing other types of tumors revealed that miR-99a and/or miR-100 are also significantly downregulated in ovarian and prostate cancer and in head and neck carcinomas (22–28). In addition, the gene encoding miR-99a lies in a region in chromosome 21q21 harboring a putative tumor suppressor gene in lung cancer (29). It is then tempting to speculate that those miRNAs play a role in the modulation of IGF-mTOR signaling also in other types of tumors.

mTOR signaling is closely interconnected with the IGF pathway because it can be activated by upstream IGF receptor signaling. mTOR activity has an essential role in the regulation of various essential cellular processes (30, 31). The protein kinase mTOR (FRAP1) has been identified as a target for rapamycin bound to FKBP12. It exists in the cell in two distinct complexes: mTORC1 and mTORC2. The two complexes have different downstream effectors and only mTORC1 is directly sensitive to rapamycin inhibition. Nevertheless, it is known that in some cell lines prolonged treatment with rapamycin also perturbs mTORC2 assembly and inhibits Akt activity (32). The relationship between the mTOR pathway and cancer is complex because, depending on the cellular context, rapamycin treatment may either inhibit cell growth or activate the oncogenic Akt kinase (33, 34). In any case, mTOR inhibition seems particularly promising as a therapeutic tool for cancers characterized by an activated Akt pathway and a relevant angiogenic component, such as ACTs (7, 35, 36). Our data show that everolimus, a rapamycin analogue, efficiently inhibits ACT cell proliferation *in vitro* and *in vivo*. In the clinical setting, it will be interesting to test the efficacy of treatments combining IGF-IR and mTOR inhibitors for the therapy of advanced adrenocortical cancer.

Here, we have shown for the first time that the mTOR and raptor proteins are direct targets for miR-99a/miR-100 inhibition in cancer cells. Interestingly, an inhibitory effect of these miRNAs on mTOR and raptor expression

was also shown during cytomegalovirus infection (37). In addition, we have revealed an unexpected mitotic localization of the active phosphorylated mTOR form (Ser^{2448}) in adrenocortical cancer cells. Phospho-mTOR staining starts to be dramatically increased at prophase among condensing chromosomes and transfers at the mitotic spindle during metaphase, being localized at the midbody during telophase and cytokinesis. Recently, a similar pattern of subcellular localization of phospho-mTOR has been described in ovarian granulosa (38) and breast cancer cells (39). These findings suggest that active mTOR signaling may have a previously unrecognized role in the regulation of mitosis and cytokinesis through phosphorylation of still undefined substrates. This hypothesis is supported by the finding that in yeast the TOR protein has been shown to affect microtubule stability and morphology and function of the mitotic spindle (40).

In the adrenal gland, activation of the mTOR pathway has also been described in a particular form of benign adrenocortical neoplasm, primary pigmented nodular adrenocortical disease (PPNAD; ref. 41). Interestingly, a recent analysis of miRNA expression in PPNAD showed that miR-100 is one of the most significantly downregulated miRNAs (42). These data suggest that a link between activated mTOR signaling and miR-100 downregulation may also exist in other types of adrenocortical neoplastic diseases.

Disclosure of Potential Conflicts of Interest

No potential conflicts of interest were disclosed.

Acknowledgments

We thank B. Mari and S. Demolombe for discussions and the gift of material, C. Ferre for help with microarray scanning, W. Rainey for the gift of HAC15 cells, F. Aguila for artwork, Novartis for the gift of RAD001, and TrGET preclinical assay platform (Canceropole PACA) for the xenograft assays.

The costs of publication of this article were defrayed in part by the payment of page charges. This article must therefore be hereby marked *advertisement* in accordance with 18 U.S.C. Section 1734 solely to indicate this fact.

Grant Support

NIH/National Cancer Institute grants CA21765 and GM083159 and American Lebanese Syrian Associated Charities (G.P. Zambetti) and Institut National du Cancer, Agence Nationale de la Recherche, Conseil Général 06, CNRS (LIA NEOGENEX) and FP7 ENS@T-CANCER (E. Lalli).

Received 10/29/2009; revised 03/03/2010; accepted 03/23/2010; published OnlineFirst 05/18/2010.

References

1. Libé R, Fratticci A, Bertherat J. Adrenocortical cancer: pathophysiology and clinical management. Endocr Relat Cancer 2007;14:13–28.
2. Michalkiewicz E, Sandrini R, Figueiredo B, et al. Clinical and outcome characteristics of children with adrenocortical tumors. An analysis of 254 cases from the International Pediatric Adrenocortical Tumor Registry. J Clin Oncol 2004;22:838–45.
3. Ribeiro RC, Sandrini F, Figueiredo B, et al. An inherited p53 mutation that contributes in a tissue-specific manner to pediatric adrenal cortical carcinoma. Proc Natl Acad Sci U S A 2001;98:9330–5.
4. Wilkin F, Gagné N, Paquette J, Oligny LL, Deal C. Pediatric adrenocortical tumors: molecular events leading to insulin-like growth factor II gene overexpression. J Clin Endocrin Metab 2000;85:2048–56.
5. Rosati R, Cerrato F, Doghman M, et al. High frequency of loss of heterozygosity at 11p15 and IGF2 overexpression is not associated with clinical outcome in childhood adrenocortical tumors positive for the R337H *TP53* mutation. Cancer Genet Cytogenet 2008;186:19–24.
6. Almeida MQ, Fragoso MC, Lotfi CF, et al. Expression of insulin-like growth factor-II and its receptor in pediatric and adult adrenocortical tumors. J Clin Endocrinol Metab 2008;93:3524–31.
7. Barlaskar FM, Spalding AC, Heaton JH, et al. Preclinical targeting of the type I insulin-like growth factor receptor in adrenocortical carcinoma. J Clin Endocrinol Metab 2009;94:204–12.
8. Doghman M, Karpova T, Rodrigues GA, et al. Increased steroidogenic factor-1 dosage triggers adrenocortical cell proliferation and cancer. Mol Endocrinol 2007;21:2968–87.
9. Doghman M, Lalli E. A matter of dosage: SF-1 in adrenocortical development and cancer. Ann Endocrinol 2009;70:148–52.
10. West A, Neale GA, Pounds S, et al. Gene expression profiling of childhood adrenocortical tumors. Cancer Res 2007;67:600–8.
11. Bartel DP. MicroRNAs: genomics, biogenesis, mechanism, and function. Cell 2004;116:281–97.
12. Garzon R, Fabbri M, Cimmino A, Calin GA, Croce CM. MicroRNA expression and function in cancer. Trends Mol Med 2006;12:580–7.
13. Calin GA, Sevignani C, Dumitru CD, et al. Human microRNA genes are frequently located at fragile sites and genomic regions involved in cancers. Proc Natl Acad Sci U S A 2004;101:2999–3004.
14. Doghman M, Arhatte M, Thibout H, et al. Nephroblastoma overexpressed/cysteine-rich protein 61/connective tissue growth factor/-nephroblastoma overexpressed gene-3 (NOV/CCN3), a selective adrenocortical cell proapoptotic factor, is down-regulated in childhood adrenocortical tumors. J Clin Endocrinol Metab 2007;92:3253–60.
15. Logié A, Boulle N, Gaston V, et al. Autocrine role of IGF-II in proliferation of human adrenocortical carcinoma NCI H295R cell line. J Mol Endocrinol 1999;23:23–32.
16. Guertin DA, Sabatini DM. Defining the role of mTOR in cancer. Cancer Cell 2007;12:9–22.
17. Parmar J, Key RE, Rainey WE. Development of an adrenocorticotropin-responsive human adrenocortical carcinoma cell line. J Clin Endocrinol Metab 2008;93:4542–6.
18. Guba M, Yezhelyev M, Eichhorn ME, et al. Rapamycin induces tumor-specific thrombosis via tissue factor in the presence of VEGF. Blood 2005;105:4463–9.
19. Lu J, Getz G, Miska EA, et al. MicroRNA expression profiles classify human cancers. Nature 2005;435:834–8.
20. Tömböl Z, Szabó PM, Molnár V, et al. Integrative molecular bioinformatics study of human adrenocortical tumors: microRNA, tissue-specific target prediction, and pathway analysis. Endocr Relat Cancer 2009;16:895–906.
21. Soon PS, Tacon LJ, Gill AJ, et al. miR-195 and miR-483-5p identified as predictors of poor prognosis in adrenocortical cancer. Clin Cancer Res 2009;15:7684–92.
22. Iorio MV, Visone R, Di Leva G, et al. MicroRNA signatures in human ovarian cancer. Cancer Res 2007;67:8699–707.
23. Yang H, Kong W, He L, et al. MicroRNA expression profiling in human ovarian cancer: miR-214 induces cell survival and cisplatin resistance by targeting PTEN. Cancer Res 2008;68:425–33.
24. Nam EJ, Yoon H, Kim SW, et al. MicroRNA expression profiles in serous ovarian carcinoma. Clin Cancer Res 2008;14:2690–5.
25. Porkka KP, Pfeiffer MJ, Waltering KK, Vessella RL, Tammela TL, Visakorpi T. MicroRNA expression profiling in prostate cancer. Cancer Res 2007;67:6130–5.
26. Tran N, McLean T, Zhang X, et al. MicroRNA expression profiles in

head and neck cancer cell lines. Biochem Biophys Res Commun 2007;358:12–7.
27. Wong TS, Liu XB, Wong BY, Ng RW, Yuen AP, Wei WI. Mature miR-184 as potential oncogenic microRNA of squamous cell carcinoma of tongue. Clin Cancer Res 2008;14:2588–92.
28. Henson BJ, Bhattacharjee S, O'Dee DM, Feingold E, Gollin SM. Decreased expression of miR-125b and miR-100 in oral cancer cells contributes to malignancy. Genes Chrom Cancer 2009;48:569–82.
29. Yamada H, Yanagisawa K, Tokumaru S, et al. Detailed characterization of a homozygously deleted region corresponding to a candidate tumor suppressor locus at 21q11-21 in human lung cancer. Genes Chrom Cancer 2008;47:810–8.
30. Hay N, Sonenberg N. Upstream and downstream of mTOR. Genes Dev 2004;18:1926–45.
31. Sarbassov DD, Ali SM, Sabatini DM. Growing roles for the mTOR pathway. Curr Opin Cell Biol 2005;17:596–603.
32. Frias MA, Thoreen CC, Jaffe JD, et al. mSin1 is necessary for Akt/PKB phosphorylation, and its isoforms define three distinct mTORC2s. Curr Biol 2006;16:1865–70.
33. O'Reilly KE, Rojo F, She QB, et al. mTOR inhibition induces upstream receptor tyrosine kinase signaling and activates Akt. Cancer Res 2006;66:1500–8.
34. Sabatini DM. mTOR and cancer: insights into a complex relationship. Nat Rev Cancer 2006;6:729–34.
35. Fassnacht M, Weismann D, Ebert S, et al. AKT is highly phosphorylated in pheochromocytomas but not in benign adrenocortical tumors. J Clin Endocrinol Metab 2005;90:4366–70.
36. de Fraipont F, El Atifi M, Gicquel C, Bertagna X, Chambaz EM, Feige JJ. Expression of the angiogenesis markers vascular endothelial growth factor-A, thrombospondin-1, and platelet-derived endothelial cell growth factor in human sporadic adrenocortical tumors: correlation with genotypic alterations. J Clin Endocrinol Metab 2000;85:4734–41.
37. Wang FZ, Weber F, Croce C, Liu CG, Liao X, Pellett PE. Human cytomegalovirus infection alters the expression of cellular microRNA species that affect its replication. J Virol 2008;82:9065–74.
38. Yaba A, Bianchi V, Borini A, Johnson J. A putative mitotic checkpoint dependent on mTOR function controls cell proliferation and survival in ovarian granulosa cells. Reprod Sci 2008;15:128–38.
39. Vazquez-Martin A, Oliveras-Ferraros C, Bernadó L, López-Bonet E, Menendez JA. The serine 2481-autophosphorylated form of mammalian target of rapamycin (mTOR) is localized to midzone and midbody in dividing cancer cells. Biochem Biophys Res Commun 2009;380:638–43.
40. Choi JH, Adames NR, Chan TF, Zeng C, Cooper JA, Zheng XF. TOR signaling regulates microtubule structure and function. Curr Biol 2000;10:861–4.
41. Mavrakis M, Lippincott-Schwartz J, Stratakis CA, Bossis I. Depletion of type IA regulatory subunit (RIα) of protein kinase A (PKA) in mammalian cells and tissues activates mTOR and causes autophagic deficiency. Hum Mol Genet 2006;15:2962–71.
42. Iliopoulos D, Bimpaki EI, Nesterova M, Stratakis CA. MicroRNA signature of primary pigmented nodular adrenocortical disease: clinical correlations and regulation of *Wnt* signaling. Cancer Res 2009;69:3278–82.